ISSN 1063-7834, Physics of the Solid State, 2016, Vol. 58, No. 11, pp. 2277–2281. © Pleiades Publishing, Ltd., 2016.
Original Russian Text © S.G. Ovchinnikov, S.N. Varnakov, S.A. Lyashchenko, I.A. Tarasov, I.A. Yakovlev, E.A. Popov, S.M. Zharkov, D.A. Velikanov, A.S. Tarasov, V.S. Zhandun, N.G. Zamkova, 2016, published in Fizika Tverdogo Tela, 2016, Vol. 58, No. 11, pp. 2195–2199.

SURFACE PHYSICS AND THIN FILMS

Iron Silicide-Based Ferromagnetic Metal/Semiconductor Nanostructures

S. G. Ovchinnikov[a, b, c, *], S. N. Varnakov[a, b], S. A. Lyashchenko[b], I. A. Tarasov[a, b], I. A. Yakovlev[b], E. A. Popov [b], S. M. Zharkov[a], D. A. Velikanov[a], A. S. Tarasov[a], V. S. Zhandun[a, b], and N. G. Zamkova[a]

[a] *Kirensky Institute of Physics, Siberian Branch, Russian Academy of Sciences, Akademgorodok 50, Building 38, Krasnoyarsk, 660036 Russia*

[b] *Reshetnev Siberian State Aero-Space University, pr. imeni Gazety "Krasnoyarskii rabochii" 31, Krasnoyarsk, 660014 Russia*

[c] *National Research Nuclear University MEPhI, Kashurskoe sh. 31, Moscow, 115409 Russia*

**e-mail: sgo@iph.krasn.ru*

Abstract—Ferromagnetic single-crystal epitaxial Fe_3Si films and polycrystalline Fe_5Si_3 films are obtained on Si substrates by molecular-beam epitaxy with in situ control of the structure, optical, and magnetic properties. The results of the structural, magnetic, and optical measurements are discussed. The experimental data are compared to the results of the microscopic calculation of the spin-polarized structure, the permittivity, and the optical conductivity spectra.

DOI: 10.1134/S1063783416110299

1. INTRODUCTION

Nanostructures based on silicon, which is the main material of modern electronics, and ferromagnetic silicides are very interesting due to the wide spectrum of their possible applications. In the last decade, epitaxial Fe_3Si films have been extensively studied to design spintronics devices [1–4]. High spin polarization of iron silicide Fe_3Si also opens possibilities for designing ferromagnetic periodic structures such as magnetophoton crystals [5]. In addition, epitaxial Fe_3Si films can be used in sensors of weak magnetic fields and as active materials of electrically controlled microwave devices due to their magnetoresonance properties [6]. Ferromagnetic silicide Fe_5Si_3 with the Curie temperature near 390 K, in its turn, is very topical for applying in thermomagnetic energy converters [7]. There are also evidence that the compound manifests the giant magnetoresistance effect due to the formation of Fe_5Si_3 nanoparticles in the silicon matrix [8]. First attempts of developing Fe/Si nanostructures have not been successful because of the formation of metal-silicide phases in the interface, which suppressed the spin-polarized transport in the semiconductor layer. Epitaxial films of various silicides such as $FeSi_2$, FeSi with CsCl, and Fe_3Si structure on Si substrates were obtained in many works [9–14]. The Mössbauer effect studies with isotopic ^{57}Fe layers were very useful for identifying various silicide phases [15]. Nevertheless, we do not know completely silicide heterostructures; the growth of heterostructure $Fe_3Si/Ge/Fe_3Si/Si(111)$ was observed in [16]. The necessity of introducing a Ge semiconductor layer instead of Si was due to lower temperature of the epitaxial growth of germanium on Fe_3Si that should not be increased to avoid uncontrolled growth of silicides in the interface. Additional interest in metal silicides is due to their significant thermoelectric properties [17]. Because of this, further studies are necessary in the field of technologies of designing silicide heterostructures and searching for new silicide phases with given magnetic and transport properties. Recently we mastered the technology of preparing single-crystal layers of ferromagnetic silicide Fe_3Si on Si(111) substrates by molecular-beam epitaxy [6] and also polycrystalline Fe_5Si_3 films [18].The equilibrium Fe_5Si_3 phase exists only at high temperatures, at which its magnetic properties are not interesting. In this work, we present the results of the measurements of the magnetic properties and the optical spectra of Fe_5Si_3 in comparison to the results of ab initio calculations of the electronic structure and various response functions, including the optical conductivity spectrum. We estimated the static conductivity. Knowledge of the electronic structure is necessary to understand the spin-polarized transport and also to form the thermoelectric properties.

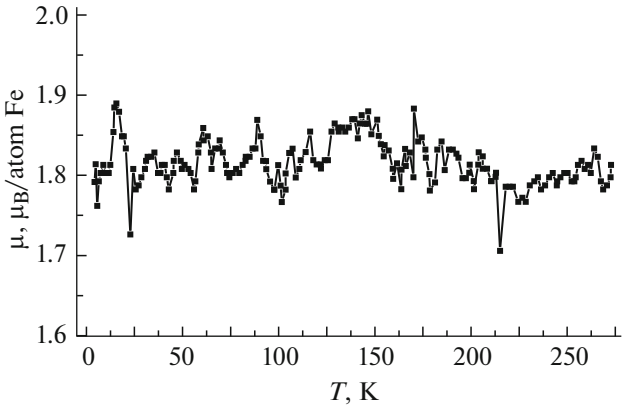

Fig. 1. Temperature dependence of the magnetization of Fe_3Si/Si in magnetic field $H = 200$ Oe.

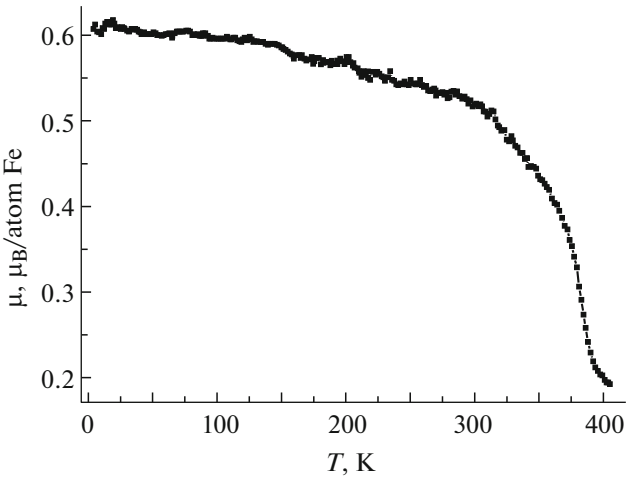

Fig. 2. Temperature dependence of the magnetization of Fe_5Si_3 in magnetic field $H = 50$ Oe.

2. PROPERTIES OF FERROMAGNETIC Fe_3Si AND Fe_5Si_3 FILMS

The single-crystal Fe_3Si film was prepared by simultaneous deposition of iron and silicon on the atomically pure surface of the Si(111) substrate (the resistivity was 5–10 Ω cm, the dopant was boron B[5]) under condition of ultrahigh vacuum in an "Angara" modernized unit of molecular-beam epitaxy. The base vacuum in the technological chamber was 6.7×10^{-8} Pa. Before synthesizing the films, the substrate was subjected to chemical treatment with subsequent thermal annealing in ultrahigh vacuum. The simultaneous sputtering of iron and silicon was performed by method of thermal evaporation from two effusion Knudsen cells made of high-temperature boron nitride. The deposition rates of individual materials were calibrated by the laser ellipsometry, which provided the ratio of the flow rates Si : Fe ≈ 0.57 that was stoichiometric for Fe_3Si. The process of formation of the structure was controlled in situ using a LEF-751M high-speed laser ellipsometer [6] and the method of reflected high-energy electron diffraction. According to the data of spectral ellipsometry, the integral thickness of the Fe_3Si layer was ~27 nm.

The polycrystalline Fe_5Si_3 was prepared by alternate deposition of subnanometer Fe and Si layers on the $SiO_2/Si(100)$ surface at a substrate temperature of 330 K in ultrahigh vacuum. The alternate deposition of the Fe and Si layers was performed by thermal evaporation from the Knudsen effusion cells. The thicknesses of each of the Fe and Si layers were 0.5–0.8 nm. The summary thickness of the Fe–Si structure was about 27 nm in conversion to the density of the bulk pure materials or 10.7 ± 0.6 μg/cm^2 for Fe and 3.1 ± 0.1 μg/cm^2 for Si. After depositing, the sample was annealed in ultrahigh vacuum at a temperature of 720 K for 30 min [18]. The X-ray diffraction study of the sample using a D8 ADVANCE powder diffractometer (Cu$K_{\alpha 1,2}$, Ni filter) with a VANTEC linear detector showed the existence of the Fe_5Si_3 phase. It should be noted that this phase exists in the bulk material only at high temperatures and is thermodynamically unstable at room temperature.

The thermodynamic dependence of the magnetization was measured using the SQUID magnetometry in the temperature range 4–400 K. The magnetization of the Fe_3Si was almost independent of temperature in this range (Fig. 1), which agrees with the Curie temperature $T_C = 850$ K. As is seen from Fig. 2, the Curie temperature of Fe_5Si_3 is much lower ($T_C \approx 390$ K).

In this work, the energy dependence of the optical conductivity was determined on the base of the data of multiangular spectral ellipsometry using the method described in detail in [19]. The calculations were carried out using the optical model of a uniform isotropic film with unknown thickness and permittivity on an isotropic Si substrate with known optical characteristics. The measurements were performed at $T = 296$ K using an Ellips-1891high-speed spectral ellipsometer.

3. SPECIFIC FEATURES OF THE ELECTRONIC STRUCTURE AND THE OPTICAL CONDUCTIVITY IN Fe_3Si AND Fe_5Si_3

The electronic structure of Fe_3Si was calculated in terms of the density functional theory in a generalized gradient approximation (GGA). The spectrum of quasi-particle excitations was obtained in both the nonself-consistent G_0W_0 approximation (G_0W_0 is the nonself-consistent mass operator with zero Green functions and the line of interaction) and various self-consistent scGW approximations (scGW is the self-consistent mass operator with "dressed" lines) without inclusion and with inclusion of peak corrections (in the form from TDDFT (the temperature-depen-

Table 1. Populations of orbitals for various position and phases in Fe_3Si

Ion	Orbital	FM		PM
		↑	↓	
Fe1	t_{2g}	0.84	0.51	0.56
(2.5μ$_B$)	e_g	0.92	0.18	0.69
Fe2	t_{2g}	0.79	0.57	0.70
(1.5μ$_B$)	e_g	0.77	0.38	0.53

FM and PM are ferromagnetic and paramagnetic phases, respectively.

Table 2. Populations of orbitals for various position and phases in Fe_5Si_3

Ion	Orbital	FM		PM
		↑	↓	
Fe1	$t_{2g}(xy)$	0.81	0.37	0.52
(1.9μ$_B$)	$t_{2g}(xz)$	0.82	0.34	0.62
	$e_g(z^2)$	0.80	0.46	0.62
	$e_g(x^2-y^2)$	0.76	0.59	0.72
Fe2	$t_{2g}(xy)$	0.74	0.58	0.66
(1.3μ$_B$)	$t_{2g}(xz)$	0.79	0.40	0.61
	$e_g(z^2)$	0.74	0.57	0.66
	$e_g(x^2-y^2)$	0.73	0.57	0.65

dence density functional theory)). In all GW variants (GW is the mass operator in the Hedin's approximation), the initial iteration step was a band structure from the GGA calculation [20]. The spectral weights of electron excitations are changed most significantly in the regions of the Brillouin band in which *d* electrons begin to contribute to the band formation. The results of the calculations in the scGW approximation best agree with the spectra of the real and imaginary parts of the permittivity and the absorption and reflection coefficients measured on our samples [20]. The magnetic state is formed by the contributions of two structurally nonequivalent iron ions. Tables 1 and 2 give the populations of various orbitals for each of positions.

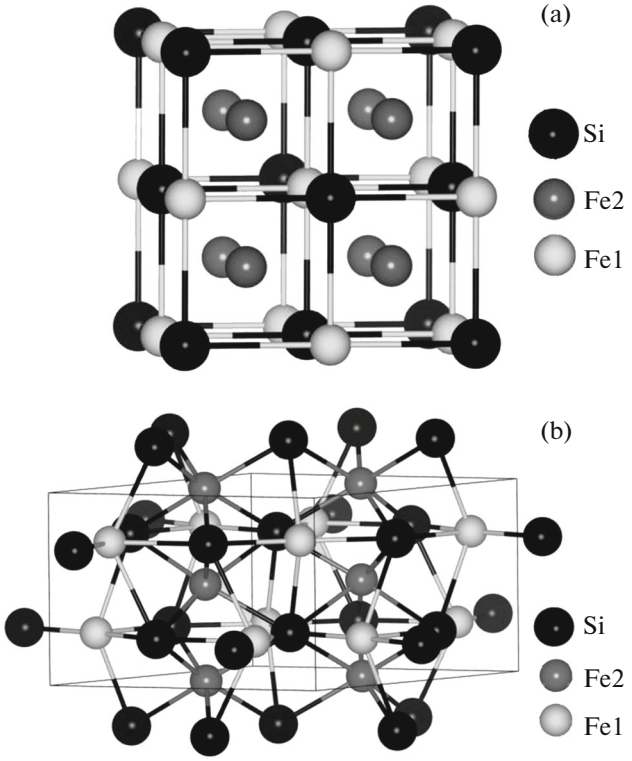

Fig. 3. Structures of (a) Fe_3Si and (b) Fe_5Si_3 with two nonequivalent iron ions.

Ions Fe1 have eight nearest neighbors Fe2 in the cubic environment and magnetic moment $M_1 = 2.52\mu_B$ (Fig. 3). Ions Fe2 are in the tetrahedral environment of Fe1 and Si ions, and their magnetic moments is $M_2 = 1.34\mu_B$. Figure 4 shows the densities of states of Fe_3Si in the ferromagnetic and paramagnetic phases singly for each of the iron positions, and the same for Fe_5Si_3 is shown in Fig. 5.

The comparison of the band structures of both silicides in the ferromagnetic and paramagnetic states showed that the transformation of the band structure at the magnetic ordering occurred more complexly than that in the simple Stoner model. At the same time, the densities of states of both silicides in the paramagnetic state had peaks at the Fermi level, which favor the fulfillment of the Stoner criterion.

4. DISCUSSION OF THE RESULTS

Figure 6 shows the spectra of the optical conductivity to compare the calculated and measured electronic properties of Fe_3Si. It is seen that the calculations qualitatively agree with the experiment at frequencies allowable in our measurements. In this frequency range, the interband transitions make the dominant contribution to the conductivity. With allowance for the intraband transitions, the low-frequency divergence is cut by the value of the static conductivity. In the framework of the band calculations, we can estimate the static conduction in the Drude–Lorentz model $\sigma_0 = (\omega_p^2\tau)/4\pi$ that uses the electronic structure parameter (plasma frequency ω_p) and one phenomenological parameter (relaxation time τ) calculated from first principles. At relaxation time $\tau = 10$ fs typical for 3*d* metals [21], for Fe_3Si we obtained static conductivity $\sigma_0 = 2.5 \times 10^6$ S/m. The conductivity mea-

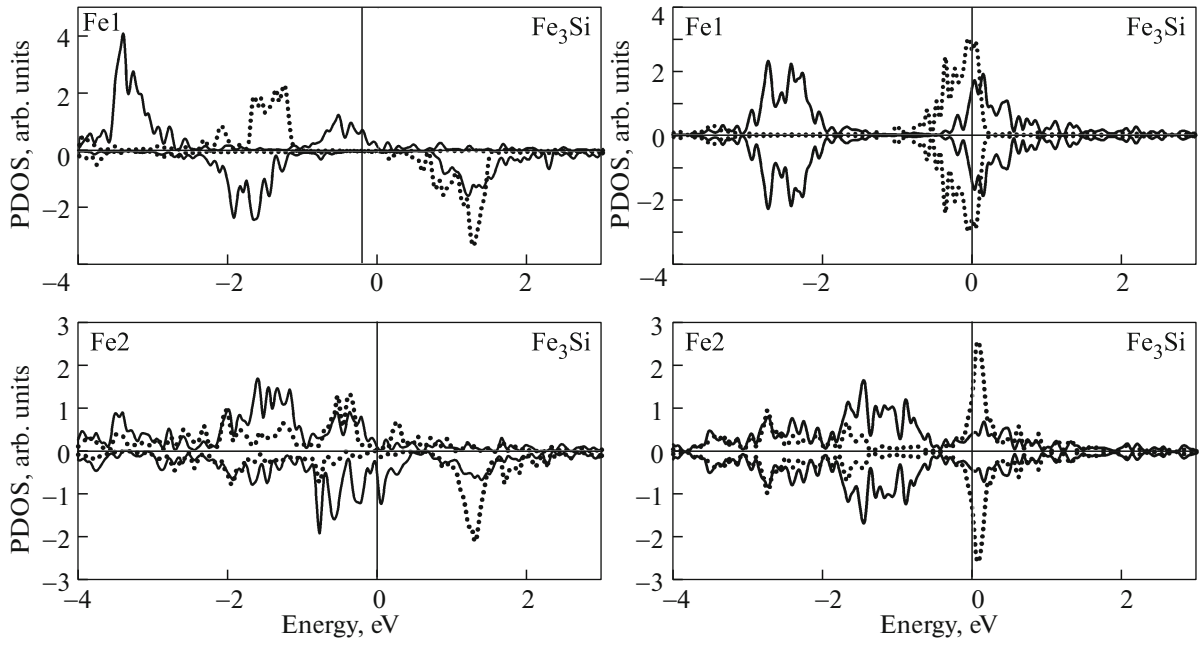

Fig. 4. Partial densities of states (PDOS) of *d* orbitals of iron in Fe_3Si. The solid line shows t_{2g} orbitals, the dotted line shows e_g orbitals, at the left in the ferromagnetic phase, and at the right in the paramagnetic phase (the GGA approximation of the density functional theory).

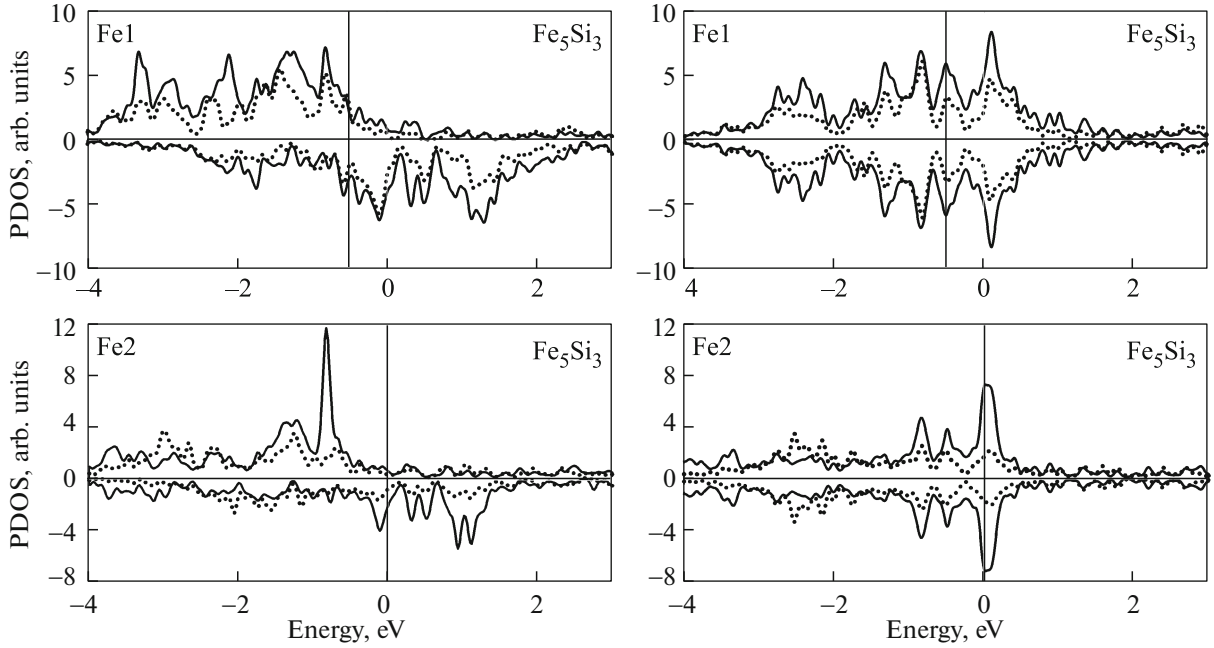

Fig. 5. Partial densities of states (PDOS) of *d* orbitals of iron in Fe_5Si_3. The solid line shows t_{2g} orbitals, the dotted line shows e_g orbitals, at the left in the ferromagnetic phase, at the right in the paramagnetic phase (the GGA approximation of the density functional theory).

sured on our samples at a temperature of 6.7 K was $\sigma_0 = 1.82 \times 10^6$ S/m. A comparison with the conductivity of pure iron 10^7 S/m shows that silicide Fe_3Si, while it is a metallic compound, has a lower conductivity than that of pure metals. The much lower Curie temperature (390 K) of the Fe_5Si_3 phase can provide

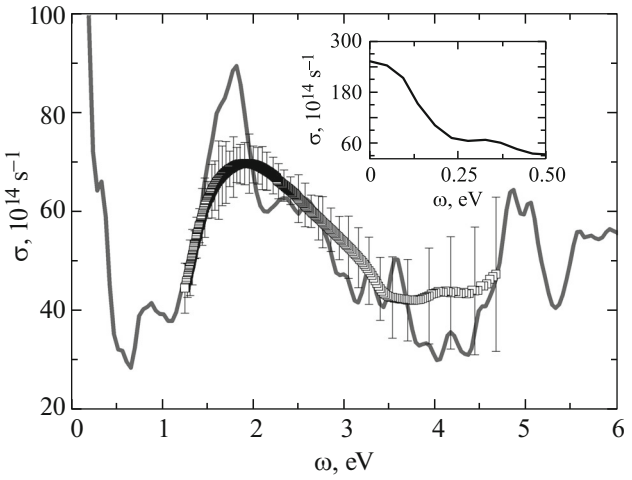

Fig. 6. Optical conductivity of Fe_3Si: (solid line) the theoretical calculation in the framework of the self-consistent scGW method and (symbols) the experimental results. The insert shows the calculated low-frequency conductivity.

larger spin fluctuations and their influence on the conductivity and the thermoelectric properties in the temperature range $T \sim 300–500$ K as compared to those of Fe_3Si.

According to the Ioffe formula for the thermoelectric quality factor, a high-quality thermoelectric material can simultaneously have high electrical conductivity, high thermopower, and low thermal conductivity. Metals have high electrical conductivity but high thermal conductivity and low thermopower. The influence of the spatial inhomogeneity in nanostructures under study provides hope on a decrease in the thermal conductivity. The thermoelectric properties of the designed nanostructures are the subject of experimental studies at the present time.

ACKNOWLEDGMENTS

The authors are very grateful to I.S. Sandalov for the useful discussion and the assistance in the interpretation of the obtained results.

This work was supported by the Russian Science Foundation, project no. 16-13-00060.

REFERENCES

1. H. Y. Hung, S. Y. Huang, P. Chang, W. C. Lin, Y. C. Liu, S. F. Lee, M. Hong, and J. Kwo, J. Cryst. Growth. **323**, 372 (2011).
2. T. Yoshitake, D. Nakagauchi, T. Ogawa, M. Itakura, N. Kuwano, Y. Tomokiyo, T. Kajiwara, and K. Nagayama, Appl. Phys. Lett. **86**, 262505 (2005).
3. Y. Ando, K. Hamaya, K. Kasahara, Y. Kishi, K. Ueda, K. Sawano, T. Sadoh, and M. Miyao, Appl. Phys. Lett. **94**, 182105 (2009).
4. Y. Fujita, S. Yamada, Y. Ando, K. Sawano, H. Itoh, M. Miyao, and K. Hamaya, J. Appl. Phys. **113**, 013916 (2013).
5. Y. Maeda, T. Ikeda, T. Ichikawa, T. Nakajima, B. Matsukura, T. Sadoh, and M. Miyao, Phys. Procedia **11**, 200 (2011).
6. I. A. Yakovlev, S. N. Varnakov, B. A. Belyaev, S. M. Zharkov, M. S. Molokeev, I. A. Tarasov, and S. G. Ovchinnikov, JETP Lett. **99** (9), 527 (2014).
7. A. Post, C. Knight, and E. Kisi, J. Appl. Phys. **114**, 033915 (2013).
8. K. S. K. Varadwaj, K. Seo, J. In, P. Mohanty, J. Park, and B. Kim, J. Am. Chem. Soc. **129**, 8594 (2007).
9. H. von Kanel, R. Stalder, H. Sirringhaus, N. Onda, and J. Henz, Appl. Surf. Sci. **53**, 196 (1991).
10. H. von Kanel, K. A. Mader, E. Muller, N. Onda, and H. Sirringhaus, Phys. Rev. B: Condens. Matter **45**, 13807 (1992).
11. E. V. Chubunova, I. D. Khabelashvili, Y. Y. Lebedinskii, V. N. Nevolin, and A. Zenkevich, Thin Solid Films **247**, 39 (1994).
12. G. J. Strijkers, J. T. Kohlhepp, H. J. M. Swagten, and W. J. M. de Jonge, Phys. Rev. B: Condens. Matter **60**, 9583 (1999).
13. M. V. Gomoyunova, D. E. Malygin, I. I. Pronin, A. S. Voronchikhin, D. V. Vyalikh, and S. L. Molodtsov, Surf. Sci. **601**, 5069 (2007).
14. H. F. Hsu, H. Y. Wu, Y. T. Huang, and T. H. Chen, Jpn. J. Appl. Phys. **48**, 08JB09 (2009).
15. M. Fanciulli, G. Weyer, H. von Kanel, and N. Onda, Phys. Scr., T **54**, 16 (1994).
16. S. Yamada, M. Miyao, and K. Hamaya, in *Proceedings of 7th International Silicon–Germanium Technology and Device Meeting (ISTDM 2014), Singapore, June 2–4, 2014*, p. 55.
17. *Thermoelectrics Handbook: Macro to Nano*, Ed. by D. M. Rowe (CRC Press, Boca Raton, Florida, 2006).
18. S. A. Lyashchenko, Z. I. Popov, S. N. Varnakov, E. A. Popov, M. S. Molokeev, I. A. YAkovlev, A. A. Kuzubov, and S. G. Ovchinnikov, J. Exp. Tech. Phys. **120** (5), 886 (2015).
19. F. K. Urban III, D. Barton, and T. Tiwald, Thin Solid Films **518**, 1411 (2009).
20. I. Sandalov, N. Zamkova, V. Zhandun, I. Tarasov, S. Varnakov, I. Yakovlev, L. Solovyov, and S. Ovchinnikov, Phys. Rev. B: Condens. Matter **92**, 205129 (2015).
21. N. Ashcroft and N. Mermin, *Solid State Physics* (Holt, Rinehart, and Winston, New York, 1976; Mir, Moscow, 1979).

Translated by Yu. Ryzhkov